Physics Letters B 664 (2008) 162–168

Contents lists available at ScienceDirect

Physics Letters B

www.elsevier.com/locate/physletb

Observation of non-exponential orbital electron capture decays of hydrogen-like ^{140}Pr and ^{142}Pm ions

Yu.A. Litvinov [a,b,*], F. Bosch [a], N. Winckler [a,b], D. Boutin [b], H.G. Essel [a], T. Faestermann [c], H. Geissel [a,b], S. Hess [a], P. Kienle [c,d], R. Knöbel [a,b], C. Kozhuharov [a], J. Kurcewicz [a], L. Maier [c], K. Beckert [a], P. Beller [✠], C. Brandau [a], L. Chen [b], C. Dimopoulou [a], B. Fabian [b], A. Fragner [d], E. Haettner [b], M. Hausmann [e], S.A. Litvinov [a,b], M. Mazzocco [a,f], F. Montes [e], A. Musumarra [g,h], C. Nociforo [a], F. Nolden [a], W. Plaß [b], A. Prochazka [a], R. Reda [d], R. Reuschl [a], C. Scheidenberger [a,b], M. Steck [a], T. Stöhlker [a,i], S. Torilov [j], M. Trassinelli [a], B. Sun [a,k], H. Weick [a], M. Winkler [a]

[a] *Gesellschaft für Schwerionenforschung GSI, 64291 Darmstadt, Germany*
[b] *Justus-Liebig Universität, 35392 Gießen, Germany*
[c] *Technische Universität München, 85748 Garching, Germany*
[d] *Stefan Meyer Institut für subatomare Physik, 1090 Vienna, Austria*
[e] *Michigan State University, East Lansing, MI 48824, USA*
[f] *Dipartimento di Fisica, INFN, I35131 Padova, Italy*
[g] *INFN-Laboratori Nazionali del Sud, I95123 Catania, Italy*
[h] *Universitá di Catania, I95123 Catania, Italy*
[i] *Ruprecht-Karls Universität Heidelberg, 69120 Heidelberg, Germany*
[j] *St. Petersburg State University, 198504 St. Petersburg, Russia*
[k] *Peking University, Beijing 100871, China*

ARTICLE INFO

Article history:
Received 17 January 2008
Received in revised form 26 February 2008
Accepted 11 April 2008
Available online 8 May 2008
Editor: V. Metag

ABSTRACT

We report on time-modulated two-body weak decays observed in the orbital electron capture of hydrogen-like $^{140}Pr^{59+}$ and $^{142}Pm^{60+}$ ions coasting in an ion storage ring. Using non-destructive single ion, time-resolved Schottky mass spectrometry we found that the expected exponential decay is modulated in time with a modulation period of about 7 seconds for both systems. Tentatively this observation is attributed to the coherent superposition of finite mass eigenstates of the electron neutrinos from the weak decay into a two-body final state.

1. Introduction

The accelerator facility of GSI Darmstadt with the heavy ion synchrotron SIS coupled via the projectile fragment separator FRS to the cooler-storage ring ESR offers a unique opportunity for decay studies of highly ionized atoms. It is possible to produce, separate, and store for extended periods of time exotic nuclei with a well-defined number of bound electrons [1]. Basic nuclear properties such as masses and lifetimes are measured by applying the mass- and time-resolved Schottky Mass Spectrometry (SMS) [2,3].

The dependance of β-lifetimes on the atomic charge state q of the parent ion has an obvious impact on our understanding of the processes ongoing in stellar nucleosynthesis [4]. Several successful experiments studying the weak decay of highly-charged ions have been performed in the past such as the experimental discovery of bound-state beta decay (β_b) of fully-ionized ^{163}Dy [5]. Due to β_b decay, fully-ionized ^{187}Re nuclei decay by 9 orders of magnitude faster than neutral atoms [6]. The first direct measurement of the ratio of bound and continuum β-decay of fully-ionized $^{207}Tl^{81+}$ was achieved by a direct observation of the decay and growth of the number of parent and daughter ions using SMS [7]. In the course of the present study the first measurements of orbital electron capture (EC) in hydrogen-like (H-like) and helium-like (He-like) ^{140}Pr ions have been performed [8,9]. It was found that the EC decay rate in H-like ^{140}Pr ions is about 50% higher than in He-like ions. This result including the measured EC/β^+ branching ratios can be explained by standard weak decay theory [10,11].

The change of the mass in a radioactive decay is evidenced by a corresponding correlated change of the revolution frequency. The area of the Schottky frequency peak is proportional to the number of stored ions and to the square of the atomic charge state, q^2. The SMS is sensitive to *single* stored ions with atomic charge states $q \geqslant 30$ [3]. However, due to a large variance in determina-

* Corresponding author at: Gesellschaft für Schwerionenforschung GSI, 64291 Darmstadt, Germany.
E-mail address: y.litvinov@gsi.de (Yu.A. Litvinov).
✠ Deceased.

0370-2693/$ – see front matter © 2008 Published by Elsevier B.V.
doi:10.1016/j.physletb.2008.04.062

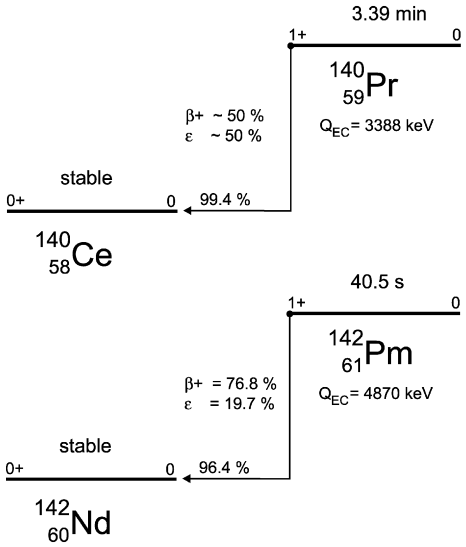

Fig. 1. Decay schemes of neutral ^{140}Pr (upper panel) and ^{142}Pm (lower panel) atoms [14].

tion of the peak areas, it became apparent that only by restricting to *three* injected parent ions at maximum one could exclude any uncertainty in the determination of the *exact* number of circulating ions. With this constraint the time of the decay of each stored ion can be precisely determined. On this basis single particle decay-spectroscopy has been developed which allows for an unambiguous and background-free identification of a certain decay branch [8,12]. This leads, however, to a very laborious collection of data which requires at least some thousand measurements to get a statistically reasonable number of decays.

Here we report on the first experiments which used time-resolved single-particle decay spectroscopy for studying the time evolution of two-body weak decays, i.e., EC and β_b-decays of radioactive ions in the ESR. The physics motivation was the question whether or not the electron neutrinos generated in such decays as coherent superposition of mass eigenstates would affect the exponential decay [13]. H-like ^{140}Pr and ^{142}Pm ions have been selected for these studies. Both nuclei decay to stable daughter nuclei via either the three-body positron emission or the two-body EC-decay. Well-known decay schemes of neutral ^{140}Pr and ^{142}Pm atoms [14] are illustrated in Fig. 1. Both systems decay mainly by a single allowed Gamow–Teller ($1^+ \rightarrow 0^+$) transition. The weak transitions to excited states can be safely neglected in our context. These nuclides have quite different decay energies (Q_{EC} values) and lifetimes, thus allowing a detailed comparison of the time evolution of the decays with different Q_{EC} and lifetimes. Both Q_{EC}-values are sufficiently large to be easily resolved by SMS. Furthermore, their half-lives are much larger than the time needed for the preparation of the ions.

2. Experiment

H-like $^{140}Pr^{58+}$ and $^{142}Pm^{60+}$ ions were produced by fragmentation of primary beams of ^{152}Sm fast extracted from the SIS with energies in the range between 500–600 MeV per nucleon. The duration of the extraction pulse was less than 1 μs which is essential since we require a well-defined time of the creation of the ions. Beryllium production targets placed at the entrance of the FRS with thicknesses of 1 and 2 g/cm^2 have been applied. The important parameters used for the experiments are summarized in Table 1. Three independent experiments were performed with Pr ions (runs 1, 2 and 3) and one with Pm ions (run 4) for comparison.

Table 1
Primary beam, target and degrader parameters, number of measurements. Each line represents a different experimental run labelled in the first column. The ion of interest is given in the second column. Energy of the ^{152}Sm primary beam E (^{152}Sm) and the thickness of the beryllium production target L (^{9}Be) are given in the third and fourth columns, respectively. The number of measurements performed in each run $\#_{inj}$ is given in the last column

Run	Ion	E (^{152}Sm) [MeV/u]	L (^{9}Be) [mg/cm^2]	$\#_{inj}$
1	$^{140}Pr^{58+}$	507.8	1032	453
2	$^{140}Pr^{58+}$	507.8	1032	842
3	$^{140}Pr^{58+}$	601.1	2513	5807
4	$^{142}Pm^{60+}$	607.4	2513	7011

The fragments of interest were separated in-flight with the FRS using the Bρ-ΔE-Bρ method [15]. For this purpose, a 731 mg/cm^2 aluminum degrader was inserted at the middle focal plane of the FRS. In runs 3 and 4 a 256 μm niobium foil after the degrader has been used in addition. In this way we separated $^{140}Pr^{58+}$ and $^{142}Pm^{60+}$ fragments without isobaric contaminations at the exit of the FRS. More details on the separation of pure $^{140}Pr^{58+}$ ions in these experiments can be found in Ref. [12].

Single bunches (less than 1 μs long) of separated ions containing on the average only two parent ions were injected into the ESR at the injection energy of 400 MeV per nucleon and then stored in the ultrahigh vacuum ($\sim 10^{-11}$ mbar). Their velocity spread caused by the production reaction was reduced within 6–10 s first by stochastic pre-cooling [16] and then by electron cooling [17] to a value of $\Delta v/v \approx 5 \times 10^{-7}$. Whereas the stochastic cooling was turned-off 5 s after each injection, the electron cooling was continuously "on" during the whole experiment at a constant and steadily monitored electron current of 50 mA. The ions coasted in the ring with a velocity of 71% of the speed of light, corresponding to a relativistic Lorentz factor $\gamma = 1.43$.

The 30th harmonic of the revolution frequency f of about 2 MHz (circumference of the ring is 108.3 m) was measured by the Fourier frequency analysis of the signals induced by the coasting ions at each revolution in pick-up plates. For cooled ions f is uniquely related to the mass-over-charge ratio M/q of the stored ions, which is the basis for the Schottky mass measurements [18]. Thus the ions of interest and their decay products could be unambiguously identified.

The data were acquired with the commercial realtime spectrum analyzer Sony-Tektronix 3066. It was triggered with the logic signal corresponding to the start event of the injection kicker of the ESR. After each trigger event, the analyzer was recording a given number of Fourier transformed noise power spectra—FFT (Fast Fourier Transform) frames. Each FFT frame had a bandwidth of 5 kHz and was collected for 128 ms. Each subsequent frame was started after a defined delay of 64 ms (runs 1, 3 and 4) or 50 ms (run 2). The recorded data were automatically stored on disk for off-line analysis.

In the ESR, the transition from the parent to the daughter ion in a nuclear decay is evidenced by a well-defined change Δf of the revolution frequency. Thus, by keeping the number of coasting ions small we could *continuously* monitor the "mass" of each ion in time and determine precisely its decay time. In our case the parent ions could have three possible fates, namely EC or β^+-decay or a loss due to atomic charge exchange reactions.

Since the atomic charge state q does *not* change in the EC-decay, Δf is determined by the mass difference (Q_{EC}-value) between the parent and daughter nuclei. The corresponding change in the revolution frequency is a few hundred Hz only (about 270 Hz for the case of ^{140}Pr and about 310 Hz for the case of ^{142}Pm at 30th harmonic). The decay is characterized by the *correlated* disappearance of the parent ion and appearance of the

daughter ion. The appearance in the frequency spectrum is delayed by 900(300) ms and 1400(400) ms for ^{140}Pr and ^{142}Pm recoiling daughter ions, respectively, needed for their cooling. The cooling times depend on both the direction and kinetic energy of the recoils. Their kinetic energies are 44 eV and 90 eV (c.m.) for the cases of ^{140}Ce and ^{142}Nd daughter nuclei, respectively. The ESR lattice and the applied ion-optical setting guarantee that *all* recoil ions still remain in the acceptance irrespective on the direction of their emission.

In β^+-decay the atomic charge changes by one unit and the frequency of the corresponding daughter ion is shifted by about −150 kHz (30th harmonic). This frequency shift is by far larger than our small observation band, and the decay is only seen by a decrease of the number of the parent ions. Such a disappearance, however, cannot be distinguished from the loss of the ion due to atomic capture or loss of an electron by reactions with the atoms of the residual gas or the electrons of the cooler. However, from the losses observed for the stable daughter ions a loss constant $\lambda_{\rm loss} \leqslant 2 \times 10^{-4}$ s^{-1} (the loss constants for H-like parent ions and fully-ionized daughter ions are almost the same [7]) could be extracted which is at least one order of magnitude smaller than the EC and β^+ decay constants $\lambda_{\rm EC}$ and λ_{β^+}, respectively. We also note that mechanical scrapers of the ESR were positioned to remove the decay products of the atomic charge-exchange reactions and the β^+-decay daughter ions.

Two out of many thousand runs are illustrated in Fig. 2 as a water-flow diagram starting at the time of the injection into the ring. These examples show one (upper panel) and two (lower panel) injected parent ions. Each horizontal line represents a frequency spectrum with 8 Hz/channel averaged over five consecutive FFT frames. The first several seconds are needed for the combined stochastic and electron cooling. The decay times are clearly seen. We emphasize that such a *continuous* observation of both the parent and daughter ions *excludes* any possible time-dependent alteration of the detection efficiency.

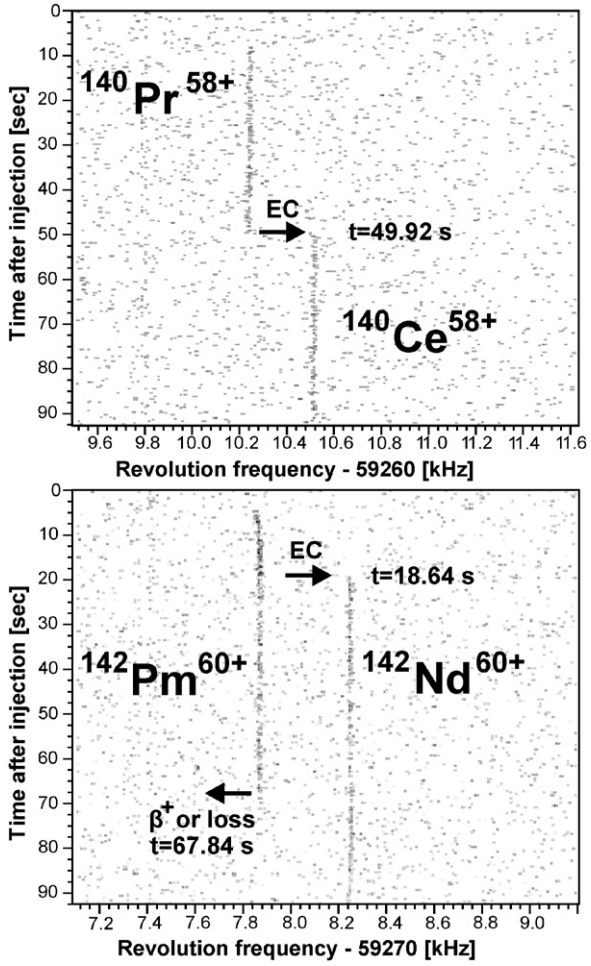

Fig. 2. Upper panel: a series of consecutive frequency spectra of a single parent ^{140}Pr^{58+} ion decaying to the daughter ^{140}Ce^{58+} ion 49.92 s after the injection into the ESR. Lower panel: two injected ^{142}Pm^{60+} ions decay 18.64 and 67.84 s after the injection. The first ion decays by electron capture to a ^{142}Nd^{60+} ion. The second ion decays by β^+-decay or is lost due to atomic charge exchange reactions. The times of the correlated disappearance of the parent ions and the appearances of EC-daughter ions are clearly seen. The first few seconds are needed for cooling. The frequency differences between parent and daughter ions correspond to $Q_{\rm EC}$ values of 3.35 and 4.83 MeV for ^{140}Pr^{58+} and ^{142}Pm^{60+} ions, respectively.

3. Data analysis and results

The aim of the analysis was to study precisely the decay characteristics of each EC-decaying ion. For this purpose, at least two independent visual and one automatic analysis have been applied to the data of each experimental run.

For achieving a better signal-to-noise ratio one may average several subsequent Schottky spectra as it is done in Fig. 2. In this way, however, one reduces the time resolution. In the visual analysis we analyzed the un-averaged FFT frames or the average over two subsequent frames. For the automatic analysis we had to average 5 FFT frames in order to achieve a sufficient signal-to-noise ratio. The details of the automatic data evaluation are described in Refs. [19,20].

The analysis was done by inspection of each FFT spectrum taken as a function of time. Then the time of appearance of a daughter nucleus following the decay of its mother was determined. It was demanded that the time values determined in independent analyses agree within less than one second. Solely the times related to the *appearance* of the time trace of the cooled daughter nuclei (see Fig. 2) were considered because they could be determined more precisely than the decay times.

The decay times from the three runs with H-like ^{140}Pr were combined. These results and the results for ^{142}Pm ions are illustrated in Fig. 3 and in Figs. 4 and 5, respectively. The time of the injection into the ESR is within 1 μs the time of the creation of the ions. The data were fitted with the exponential decay function:

$$\frac{dN_{\rm EC}(t)}{dt} = N(0) \cdot \lambda_{\rm EC} \cdot e^{-\lambda t}, \tag{1}$$

where $N(0)$ is the number of parent ions at the time $t = 0$, the time of injection and $\lambda = \lambda_{\rm EC} + \lambda_{\beta^+} + \lambda_{\rm loss}$. The ratio of $\lambda_{\rm EC}/\lambda_{\beta^+}$ is 0.95(8) for the H-like ^{140}Pr and is expected to be about 0.32 for the H-like ^{142}Pm [9].

It is clear to see that the expected exponential decrease of the EC-decays as a function of time shows a superimposed periodic time modulation. To account for this modulation we fitted the data with the function:

$$\frac{dN_{\rm EC}(t)}{dt} = N(0) \cdot e^{-\lambda t} \cdot \widetilde{\lambda_{\rm EC}}(t), \tag{2}$$

where $\widetilde{\lambda_{\rm EC}}(t) = \lambda_{\rm EC} \cdot [1 + a \cdot \cos(\omega t + \phi)]$ with an amplitude a, an angular frequency ω, and a phase ϕ of the modulation. For the case of ^{142}Pm ions only the first 33 seconds after the injection were fitted with Eq. (2) due to the short half-life of the mother nuclei and, thus, the fast damping of the modulation amplitude.

The fits were done with the MINUIT package [21] using the χ^2 minimization and the maximum likelyhood methods which yielded consistent results. The fit parameters are given in Table 2.

The total decay constants λ obtained from both fitting functions (Eqs. (1) and (2)) agree within their error margins for the ^{140}Pr data and for the ^{142}Pm data with a fit up to 33 seconds

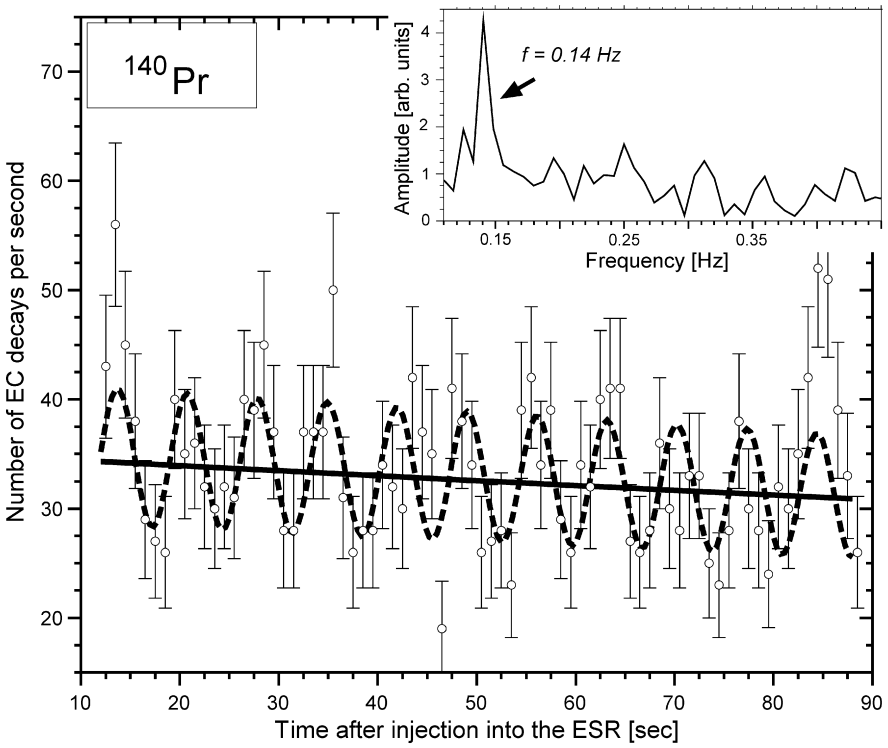

Fig. 3. Number of EC-decays of H-like ^{140}Pr ions per second as a function of the time after the injection into the ring. The solid and dashed lines represent the fits according to Eq. (1) (without modulation) and Eq. (2) (with modulation), respectively. The inset shows the Fast Fourier Transform of these data. A clear frequency signal is observed at 0.14 Hz (laboratory frame).

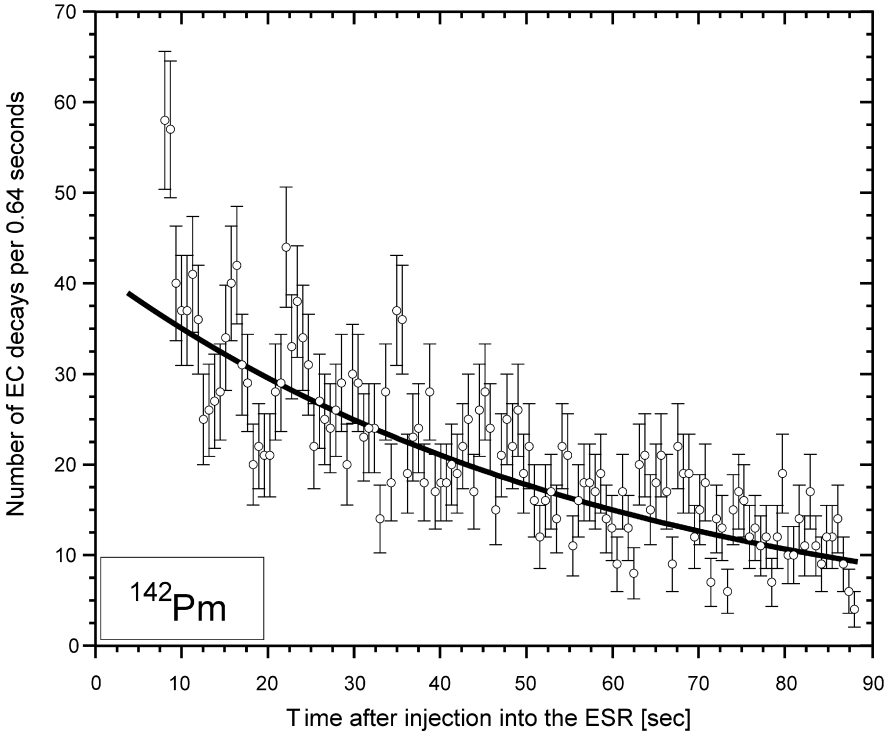

Fig. 4. Number of EC-decays of H-like ^{142}Pm ions per 0.64 seconds as a function of the time after the injection into the ring. The solid line shows the exponential decay fit according to Eq. (1).

after injection. We note that the decay constants of pure exponential decay obtained from *all* ^{142}Pm data points and from data points until 33 seconds after injection differ by nearly 1.5 standard deviations. The decay constants for the ^{140}Pr data have large uncertainties which are conceivable because the number of EC-decays per second decreases by less than 10% within the total observation time. All deduced decay constants agree within two standard deviations with the corresponding literature values for neutral atoms [14] corrected for missing electrons and taking into account the observed "enhancement" of the EC-decay in H-like ions [9].

From the angular frequencies ω of Table 2 we extract the periods of the modulation as 7.06(8) and 7.10(22) s (laboratory frame)

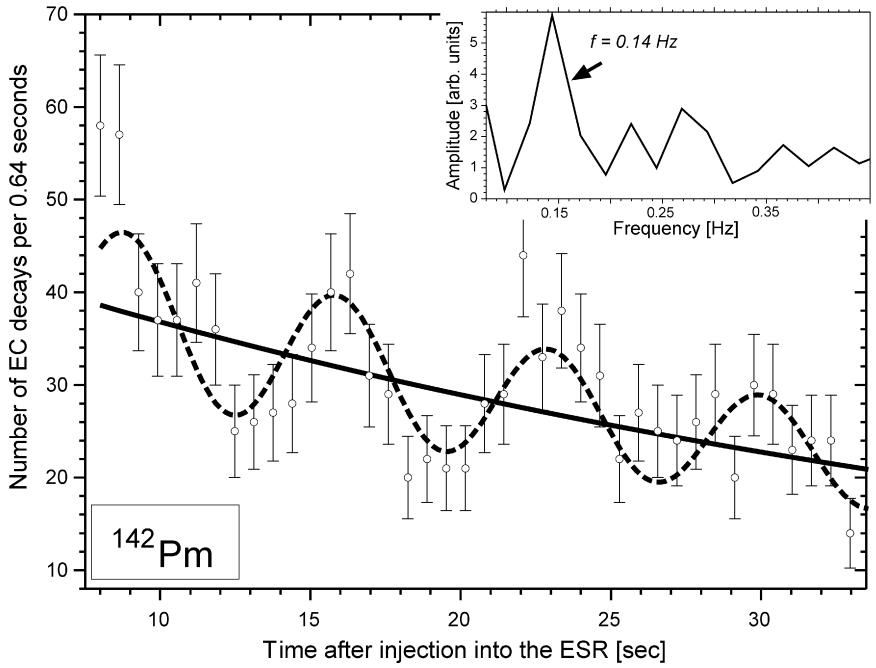

Fig. 5. A zoom to the first 33 s after injection of the ^{142}Pm data presented in Fig. 4. The solid line represents the exponential decay fit according to Eq. (1). The dashed line shows the fit according to Eq. (2). Both fits were done until 33 s after injection and are marked with an asterisk in Table 2. The inset shows the FFT spectrum obtained from these data. A clear FFT peak is observed at about 0.14 Hz (laboratory frame). Its reduced resolution as compared to the corresponding FFT in Fig. 3 is explained by the smaller number of points used.

Table 2
The fit parameters for the total decay constant λ, the amplitudes a, the (angular) frequencies ω, and the phases ϕ are summarized for ^{140}Pr (upper part) and ^{142}Pm (lower part) EC-decay data illustrated in Figs. 3, 4 and 5. The fits are done according to Eqs. (1) and (2) which is indicated in the first column. The corresponding χ^2/DoF (DoF = degrees of freedom) are given in the last column. The results of the fits for the ^{142}Pm data until 33 seconds after injection are marked with an asterisk (last two rows). All values for λ and ω are referred to the laboratory system (relativistic Lorentz factor $\gamma = 1.43$)

Fit parameters of ^{140}Pr data						
Eq.	$N_0\lambda_{EC}$ [s^{-1}]	λ [s^{-1}]	a	ω [s^{-1}]	ϕ	χ^2/DoF
(1)	34.9(18)	0.0014(10)	–	–	–	107.2/73
(2)	35.4(18)	0.0015(10)	0.18(3)	0.890(11)	0.4(4)	67.18/70
Fit parameters of ^{142}Pm data						
Eq.	$N_0\lambda_{EC}$ [s^{-1}]	λ [s^{-1}]	a	ω [s^{-1}]	ϕ	χ^2/DoF
(1)	41.5(17)	0.0170(9)	–	–	–	173/124
(1)	46.8(40)*	0.0240(42)*	–	–	–	63.77/38*
(2)	46.0(39)*	0.0224(42)*	0.23(4)*	0.885(31)*	−1.6(5)*	31.82/35*

for ^{140}Pr and ^{142}Pm ions, respectively. The presence of the modulation frequencies was also confirmed by Fast Fourier Transforms (see insets in Figs. 3 and 5).

The amplitudes a of the periodic modulation agree within the error margins. The average value of both systems is $\langle a \rangle = 0.20(2)$. Although the ansatz of damping factor for the amplitudes might further improve the fit quality, we refrain from presenting such an analysis because of the still scarce counting statistics.

The fit results for the phases ϕ of the ^{140}Pr and ^{142}Pm data reflect the different times needed to cool the recoiling ^{140}Ce (900 ms) and ^{142}Nd (1400 ms) daughter ions with kinetic energies of 44 and 90 eV, respectively.

4. Discussion

The observed periodic modulations of the expected exponential decrease of the number of EC-decays per time unit still suffer from restricted statistics. However, the "zero hypothesis" of a pure exponential decay can be already rejected according to the χ^2/DoF-values from Table 2 on the 99% confidence level (one-sided probabilities $p = 0.006$) for both investigated nuclear systems.

First of all, the finding of nearly the same oscillation period of about 7 s might suggest a technical artefact as their common origin, such as periodic instabilities in the storage ring or of the recording systems. However, this explanation is very improbable due to our detection technique where we have—during the whole observation time—*the complete and uninterrupted information upon the status of each stored ion*. Furthermore, the parent and daughter ions from both systems coast on different orbits in the ESR and have different circulation times. We can also exclude binning effects or the variance of the delay between the decay of the mother and the "re-appearance" of the daughter ion, since these effects lead to an uncertainty of the decay time that is much smaller than the observed period.

It is very probable that the H-like ^{140}Pr as well as the ^{142}Pm ions with nuclear spin $I = 1^+$ are produced in a coherent superposition of the two 1s hyperfine states with total angular momenta $F = 1/2$ and $F = 3/2$. This could lead to well-known quantum beats with a beat period $T = h/\Delta E$, where ΔE is the hyperfine splitting. However, those beat periods should be more than twelve orders of magnitude shorter than the observed ones.

The weak decay conserves the F quantum number, and since the final state (fully ionized daughter nuclei with $I = 0^+$ and emitted electron neutrino ν_e) has $F = 1/2$, the EC-decay from the $F = 3/2$ state is *not* allowed [8,9]. Only a hypothetical, yet unknown, mechanism which transfers the parent ions *periodically* within 7 seconds from the $F = 1/2$ ground state (for positive magnetic moment [9]) to the "sterile" $F = 3/2$ state and back in both nuclides could generate the observed modulations [22].

First of all, one could think on steady population changes of the two hyperfine states caused by the time-dependent electric fields as the ions move at 71% of light velocity, or on periodic changes of the vacuum in the ESR or, in particular, on spin-flip processes due to the steady interaction of the parent nuclei with the

electrons of the cooler. It is unknown whether the spin-flip probability λ_{flip} from the interaction with the slowly co-moving cooler electrons could reach the interesting region of $\lambda_{\text{flip}} \approx 0.1 \ldots 1\ \text{s}^{-1}$, becoming comparable to a decay probability λ_{dec} from the upper hyperfine level in the order of $\lambda_{\text{dec}} \approx 0.1 \ldots 1\ \text{s}^{-1}$. However, this would only lead–after a time of the order of $\max[1/\lambda_{\text{flip}}, 1/\lambda_{\text{dec}}]$—to a *stationary* population of the two levels. Only a significant, periodic change of λ_{flip} (caused, e.g., by a periodically changing electron current) could effect the periodic change of the EC-decay probability. From our continuous monitoring of the electron current and of the vacuum in the ring we have no hint on such periodic changes. Moreover, the ESR vacuum system is almost completely decoupled from the vacuum systems of the SIS and FRS which excludes any (periodic) influences from these devices.

The most striking argument against such periodic transfers from/to the "sterile" state is that the total decay probability should be *reduced* which is not in agreement with corresponding decay measurements of many stored ions [7,9].

Thus, we try to interpret the modulations as due to the properties of the electron neutrino that is generated in the EC-decay as a coherent superposition of at least two mass eigenstates. This necessarily comprises that also the recoiling daughter nuclei appear as a coherent superposition of states that are entangled with the electron neutrino mass eigenstates by momentum- and energy conservation.

We note that a time structure was observed in the two-body decay of stopped pions in KARMEN experiment (KARMEN time anomaly) [23]. This anomaly was described in Ref. [24] by using a function containing periodic time modulation similar to Eq. (2).

There is a long-lasting and still persisting debate whether the generated neutrino mass eigenstates should have the same energy or rather the same three-momentum $\vec{q}_\nu$ or neither of them [25–29]. In our case, this question can be addressed properly only in the context of wave-packets since we observe the decaying system in a restricted region of space and time. This necessarily generates an uncertainty of both momentum and energy. An attempt to interpret the modulation times in this framework has been made in Ref. [30].

Disregarding momentum and energy spread in a simplified picture and restricting to two neutrino mass eigenstates, one gets from momentum and energy conservation for an initial state with energy E and momentum $\mathbf{P} = 0$ in the c.m. system[1]:

$$E_1 + M + \frac{p_1^2}{2M} = E, \tag{3}$$

$$E_2 + M + \frac{p_2^2}{2M} = E, \tag{4}$$

where $E_i = \sqrt{p_i^2 + m_i^2}$ denotes the energy of the two neutrino mass eigenstates with masses m_1 and m_2, respectively, $p_i^2/2M$ the corresponding kinetic energies of the recoiling daughter nuclei, and where M is the mass of the daughter nucleus. By combining these two equations and neglecting a term given by the ratio of the recoil energy and the mass of the daughter nucleus we arrive at (see, e.g., Refs. [31,32]):

$$\Delta E = E_2 - E_1 \approx \frac{\Delta m^2}{2M}, \tag{5}$$

where $\Delta m^2 = m_2^2 - m_1^2$.

The modulations could be caused by the energy splitting ΔE which is indicated by almost the same observed modulation periods for both decaying nuclei ^{140}Pr and ^{142}Pm with almost the same nuclear masses M but with quite different neutrino energies and, thus, momenta. One expects for a mass of 140 mass units and for $\Delta m^2 \approx 10^{-4}$ eV^2 [33] a period in the c.m. system of roughly $T = 10$ s. Besides the fact that this estimate is based on several assumptions many questions remain. How could the coherence of the entangled quantum states be preserved over time spans of some ten seconds? What is the effect of the continuous monitoring of the state of the ion? Is the "phase" between the entangled neutrino mass eigenstates set back to zero at each observation?

It is obvious that our findings must be corroborated by the study of other two-body beta decays (EC and β_b). Furthermore, it has to be investigated how the oscillation period—if persisting at all—depends on the nuclear mass M. Mandatory are also investigations of three-body β-decays, where oscillations should be washed out due to the broad distribution of neutrino (sc. recoil) energies. Finally, an interesting case arises when the decaying nucleus is not free, but couples to the full phonon spectrum in the lattice of a solid.

[1] In the following we set $c = 1$.

Acknowledgements

We would like to express our deep gratitude to W. Henning for his continuous support and invaluable advice. It is a pleasure to acknowledge many fruitful and engaged discussions with L. Batist, K. Blaum, P. Braun-Munzinger, H. Emling, A. Fäßler, B. Franzke, S.J. Freedman, L. Grigorenko, A. Ivanov, H.-J. Kluge, E. Kolomeitsev, R. Krücken, M. Lindner, M. Lindross, G. Münzenberg, Z. Patyk, K. Riisager, A. Schäfer, J. Schiffer, D. Schwalm, R. Schuch, N. Severijns, H. Stöcker, P.M. Walker, J. Wambach, and H. Wilschut. We would like to thank in particular H. Feldmeier, M. Kleber, K.H. Langanke, H. Lipkin, P. Vogel, Ch. Weinheimer, and K. Yazaki for intensive theoretical discussions. We are grateful to Th. Müller and A. Le Fèvre for the help in the data evaluation. We are indebted to the HADES and IKAR Collaborations for their help and flexibility concerning the beam time schedule. The excellent support by the accelerator team of GSI decisively contributed to the successful achievement of our experiments. One of us (M.T.) acknowledges the support by the A. von Humboldt Foundation.

References

[1] H. Geissel, et al., Phys. Rev. Lett. 68 (1992) 3412.
[2] T. Radon, et al., Phys. Rev. Lett. 78 (1997) 4701.
[3] Yu.A. Litvinov, et al., Nucl. Phys. A 756 (2005) 3.
[4] K. Takahashi, K. Yokoi, Nucl. Phys. A 404 (1983) 578.
[5] M. Jung, et al., Phys. Rev. Lett. 69 (1992) 2164.
[6] F. Bosch, et al., Phys. Rev. Lett. 77 (1996) 5190.
[7] T. Ohtsubo, et al., Phys. Rev. Lett. 95 (2005) 052501.
[8] H. Geissel, et al., Eur. Phys. J., Special Topics 150 (2007) 109.
[9] Yu.A. Litvinov, et al., Phys. Rev. Lett. 99 (2007) 262501.
[10] Z. Patyk, et al., Phys. Rev. C 77 (2008) 014306.
[11] A.N. Ivanov, M. Faber, R. Reda, P. Kienle, arXiv: 0711.3184 [nucl-th], Phys. Lett. B (2008), in press.
[12] Yu.A. Litvinov, et al., nucl-ex/0509019.
[13] Yu.A. Litvinov, F. Bosch, et al., Experimental proposal for SIS-FRS-ESR facilities E077, GSI, Darmstadt, 2006.
[14] R.B. Firestone, et al., Table of Isotopes, eighth ed., Willey, New York, 1999.
[15] H. Geissel, et al., Nucl. Instrum. Methods B 70 (1992) 286.
[16] F. Nolden, et al., Nucl. Instrum. Methods A 532 (2004) 329.
[17] M. Steck, et al., Nucl. Instrum. Methods A 532 (2004) 357.
[18] T. Radon, et al., Nucl. Phys. A 677 (2000) 75.
[19] H.G. Essel, GSI Scientific Report 2006, GSI Report 2007-1, 2007, p. 205.
[20] N. Winckler, Doctoral Thesis, JLU Giessen, in preparation.
[21] Function Minimization and Error Analysis (MINUIT), CERN Program Library, Computing and Network Division, CERN Geneva, Switzerland; http://wwwasdoc.cern.ch/wwwasdoc/minuit/minmain.html.
[22] Ch. Weinheimer, L. Grigorenko, E. Kolomeitsev, 2007, private communications.
[23] B. Armbruster, et al., Phys. Lett. B 348 (1995) 19.
[24] Y.N. Srivastava, et al., hep-ph/9807543.

[25] S. Bilenky, B. Pontecorvo, Phys. Rep. C 41 (1978) 225.
[26] B. Kayser, Phys. Rev. D 24 (1981) 110.
[27] A.D. Dolgov, A.Yu. Morozov, L.B. Okun, M.G. Schepkin, Nucl. Phys. B 502 (1997) 3.
[28] L. Stodolsky, Phys. Rev. D 58 (1998) 036006.
[29] H.J. Lipkin, Phys. Lett. B 579 (2004) 355.
[30] A.N. Ivanov, R. Reda, P. Kienle, arXiv: 0801.2121 [nucl-th];
A.N. Ivanov, E. Kryshen, M. Pitschmann, P. Kienle, arXiv: 0804.1311 [nucl-th].
[31] J. Lowe, et al., hep-ph/9605234.
[32] Y. Srivastava, A. Widom, E. Sassaroli, Eur. Phys. J. C 2 (1998) 769.
[33] KamLAND Collaboration, Phys. Rev. Lett. 94 (2005) 081801.